Chem. Mater. **2007,** *19,* 2007−2015

Buckling Behavior of Highly Oriented Silver Nanowires Encapsulated within Layer-by-Layer Films

Ray Gunawidjaja, Hyunhyub Ko, Chaoyang Jiang, and Vladimir V. Tsukruk*

School of Materials Science and Engineering, Georgia Institute of Technology, Atlanta, Georgia 30332

Received December 19, 2006. Revised Manuscript Received February 14, 2007

Unidirectionally oriented silver nanowires encapsulated into a nanoscale polymeric film result in anisotropic mechanical response of the composite film with much stiffer (fivefold) properties in the direction of nanowire orientation. This difference is caused by the fact that under a longitudinal compressive stress (parallel to the direction of orientation), the individual nanowires undergo the buckling process, thus, contributing into the higher composite stiffness of the film. This matrix-induced buckling phenomenon can be used as a fast and straightforward method of measuring the elastic modulus of the metallic nanowires from the buckling spacing with good precision. Using Euler's equation for the buckling instability of a slender column, the Young's modulus of silver nanowires was determined to be 118 ± 14 GPa, which is higher than that of the bulk silver but falls within the range of values obtained with other independent measurements.

Introduction

Uniformly oriented assembly of one-dimensional (1D) nanostructures can lead to novel anisotropic physical properties. For instance, oriented arrays of silver nanowires (AgNWs) can serve as an excellent substrate for surface enhanced Raman scattering (SERS).[1,2] The polarization effect is also observed for its UV extinction spectra. For gold nanorods, the small size and the polarization effect make them ideal for plasmon-based optical sensing material.[3,4] Recently, plasmon propagation along the silver and gold nanowires was reported, thus making them good candidates for photonic or guide fiber applications as well.[5−8] Furthermore, it has been demonstrated that unidirectional carbon nanotube composites can exhibit significant electrical and mechanical anisotropy.[9,10] In another example, Jin et al. demonstrated silicon nanowire utilization for the fabrication of a field-effect transistor.[11,12] For applications where the directional mechanical load matters, anisotropic reinforced nanocomposites can be tailored to ensure a greater strength-to-weight ratio. However, a uniform alignment of nanorods or nanowires is a challenging task and is rarely achieved by using traditional processing approaches.[13]

Thus, there are currently limited accounts on incorporating 1D nanoparticles (especially in a highly oriented state) into ultrathin polymeric films which can be free-standing.[14] The ability to freely suspend 1D nanoparticles bears potential in thermal, acoustic, and chemical sensing applications that demand miniaturizations and enhanced capabilities.[15−18] Despite numerous techniques put forth to assemble 1D nanoparticles within ultrathin composite films in an anisotropic manner, the uniform orientation combined with a high density of packing is rarely achieved.[19−21] In one of the successful examples, the Langmuir−Blodgett (LB) technique was demonstrated as a powerful tool which enables controlled density and inter-particle distance, but this approach cannot be easily used for the fabrication of stable nanoscale polymeric films.[22]

Here, we focus on fabricating uniformly oriented AgNWs encapsulated into a flexible and ultrathin polymeric film which is robust enough to exist in the free-standing state without need for a supporting solid substrate. In doing so, we considered two different methods for nanowire orienta-

---

* To whom correspondence should be addressed. Tel.: 404-894-6081. Fax: 404-894-9140. E-mail: vladimir@mse.gatech.edu.

(1) Tao, A.; Kim, F.; Hess, C.; Goldberger, J.; He, R.; Sun, Y.; Yang, P. *Nano Lett.* **2003**, *3*, 1229.
(2) Jeong, D. H.; Zhang, Y. X.; Moskovitos, M. *J. Phys. Chem. B* **2004**, *108*, 12724.
(3) Sönnichsen, C.; Alivisatos, A. P. *Nano Lett.* **2005**, *5*, 301.
(4) Murphy, C. J.; Sau, T. K.; Gole, A. M.; Orendorff, C. J.; Gao, J.; Gou, L.; Hunyadi, S. E.; Li, T. *J. Phys. Chem. B* **2005**, *109*, 13857.
(5) Dickson, R. M.; Lyon, L. A. *J. Phys. Chem. B* **2000**, *104*, 6095.
(6) Graff, A.; Wagner, D.; Ditlbacher, H.; Kreibig, U. *Eur. Phys. J. D* **2005**, *34*, 263.
(7) Sanders, A. W.; Routenberg, D. A.; Wiley, B. J.; Xia, Y.; Dufresne, E. R.; Reed, M. A. *Nano Lett.* **2006**, *6*, 1822.
(8) Maier, S. A.; Kik, P. G.; Atwater, H. A.; Meltzer, S.; Harel, E.; Koel, B. E.; Requicha, A. A. *Nat. Mater.* **2003**, *2*, 229.
(9) Du, F.; Fischer, J. E.; Winey, K. I. *Phys. Rev. B.* **2005**, *72*, 121404.
(10) Thostenson, E. T.; Chou, T.-W. *Carbon* **2004**, *42*, 3003.
(11) Whang, D.; Jin, S.; Wu, Y.; Lieber, C. M. *Nano Lett.* **2003**, *3*, 1255.
(12) Jin, S.; Whang, D.; McAlpine, M. C.; Friedman, R. S.; Wu, Y.; Lieber, C. M. *Nano Lett.* **2004**, *4*, 915.
(13) Kim, F.; Kwan, S.; Akana, J.; Yang, P. *J. Am. Chem. Soc.* **2001**, *123*, 4360.
(14) Jiang, C.; Tsukruk, V. V. *Adv. Mater.* **2006**, *18*, 829.
(15) Jiang, C.; Markutsya, S.; Pikus, Y.; Tsukruk, V. V. *Nat. Mater.* **2004**, *3*, 721.
(16) Jiang, C.; Kommireddy, D. S.; Tsukruk, V. V. *Adv. Funct. Mater.* **2006**, *16*, 27.
(17) Markutsya, S.; Jiang, C.; Pikus, Y.; Tsukruk, V. V. *Adv. Funct. Mater.* **2005**, *15*, 771.
(18) Jiang, C.; McConney, M. E.; Singamaneni, S.; Merrick, E.; Chen, Y.; Zhao, J.; Zhang, L.; Tsukruk, V. V. *Chem. Mater.* **2006**, *18*, 2632.
(19) Pérez-Juste, J.; Pastoriza-Santos, I.; Liz-Marzán, L. M.; Mulvaney, P. *Coord. Chem. Rev.* **2005**, *249*, 1870.
(20) Gupta, S.; Zhang, Q.; Emrick, T.; Russell, T. P. *Nano Lett.* **2006**, *6*, 2066.
(21) Nikoobakht, B.; Wang, Z. L.; El-Sayed, M. A. *J. Phys. Chem. B* **2000**, *104*, 8635.
(22) Fendler, J. H. *Chem. Mater.* **1996**, *8*, 1616.

10.1021/cm063022e CCC: $37.00 © 2007 American Chemical Society
Published on Web 03/24/2007

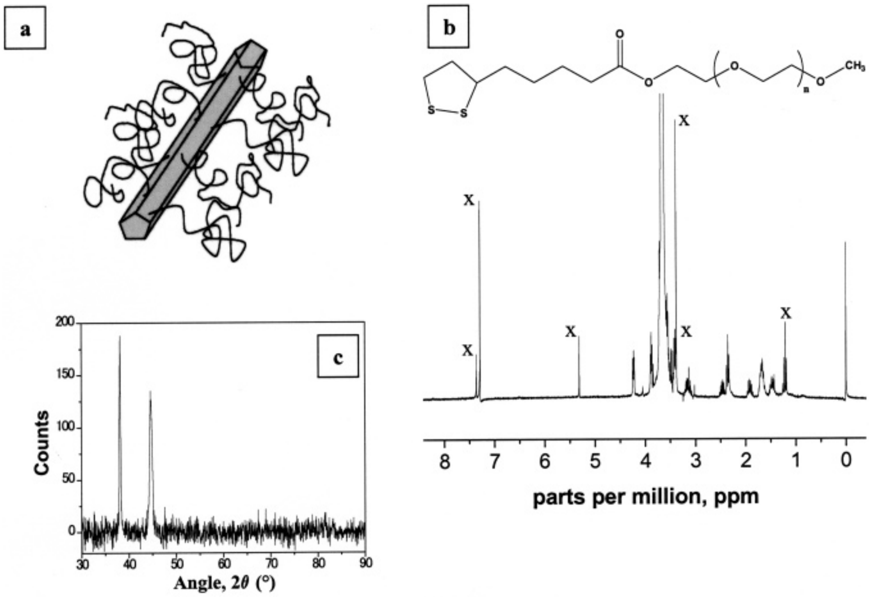

Figure 1. (a) Purified polyol synthesized AgNW with PVP on surface. (b) ^{1}H NMR spectrum of poly(ethylene glycol) methyl ether DL-6,8-thioctate. "x" designate traces of solvent (benzene, diethyl ether, chloroform, dichloromethane, and methanol). (c) X-ray diffraction spectrum of Ag-PEO on a glass substrate.

tion: fine control of the microfluidic flow via microcontact printing and the directional compression of a Langmuir monolayer. Highly oriented nanowires were obtained in both cases, and the resulting uniform arrays were encapsulated into polyelectrolyte layer-by-layer (LbL) films. Their highly anisotropic mechanical properties were revealed with a buckling test. An interesting phenomenon of polymer matrix-induced longitudinal buckling of AgNWs observed here was utilized for a fast and straightforward measurement the elastic modulus of these nanowires.

Experimental Section

Chemicals and Materials. All chemicals were purchased from Aldrich and used without further purification. AgNWs were synthesized in a high yield and purified according to the well-known procedure using $AgNO_3$ precursor and poly(vinylpyrrolidone) (PVP) as a capping agent ($M_n = 1.3 \times 10^6$ Da) in accordance with the literature data (Figure 1a).[23] For LB deposition, a portion of the solution was treated with poly(ethylene glycol) methyl ether DL-6,8-thioctate by stirring the mixture in methanol (4% water) for 1 week to yield Ag-PEO. In 60 mL of methanol, 1.3 g of DL-6,8-thioctyl ester PEO was used for 67 mg of AgNWs (estimated mass). From here onward, the notation Ag-PEO will be used throughout the manuscript to denote poly(ethylene glycol) methyl ether DL-6,8-thioctate treated AgNWs. Ag-PEO material was isolated by multiple filtrations through a nylon filter (pore size 5 μm) and re-dispersed in an excess volume of methanol. Finally, Ag-PEO material was dispersed in chloroform (HPLC grade) to give a concentration of 3 mg/mL. The gray-silhouette Ag-PEO solution precipitates over time; thus, a brief sonication treatment was necessary prior to each LB deposition.

Poly(ethylene glycol) methyl ether DL-6,8-thioctate (5000 Da) was synthesized as follows: poly(ethylene glycol) methyl ether (5 g, 1 equiv) solution in 55 mL of benzene was first refluxed in a dean-stark flask to remove water. After reflux, there was approximately 25−30 mL of benzene left in a flask. The solution was cooled in an ice bath before 4-dimethylaminopyridine, 4-DMAP (30.5 mg, 0.25 equiv), and DL-6,8-thioctic acid (268 mg, 1.3 equiv) were added under stirring. Finally *N*,*N*′-dicyclohexylcarbodiimide, DCC (268 mg, 1.3 equiv), dissolved in a minimum amount of dry benzene was added. The solution was allowed to stir for 24 h. The product of hydration, dicyclohexylurea (DCU) white precipitate, was first removed by centrifugation at 7000 rpm. Next, poly(ethylene glycol) methyl ether DL-6,8-thioctate was isolated by the precipitation in diethyl ether (yield about 70%). The chemical structure of the dry powder was confirmed using a proton nuclear magnetic resonance technique, ^{1}H NMR (δ, ppm, $CDCl_3$). The chemical structure shown in Figure 1b was confirmed by NMR as follows: 1.4−1.55 (m, 2H), 1.55−1.80 (m, 4H), 1.85−2.0 (m, 1H), 2.35 (t, 2H), 2.40−2.55 (m, 1H), 3.05−3.25 (m, 2H), 3.65 (s, 310H), 3.88 (t, 2H), 4.23 (s, 2H).

X-ray diffraction for Ag-PEO shows the (111) and (200) reflections at 38.15° and 44.45°, respectively, which correspond to the face-centered cubic unit cell (FCC) with $a = 0.408$ nm (Figure 1c).[24,25] As has been discussed in the literature, AgNWs synthesized by this procedure possess a pentagonal cross section bounded by the [100] planes and capped by the [111] facets on both ends with the growth direction along the [110] vector.[26] The "molecular weight" of a single AgNW, 1.62×10^{11} Da, was estimated from their dimensions (length, 6.1 ± 2 μm, and diameter, 75 ± 10 nm, as reported in our recent publication), and the unit cell parameters were determined from the X-ray data.[23]

Techniques and Instrumentation. ^{1}H NMR spectra were obtained using a 300 MHz Bruker spectrometer. UV/vis spectra were recorded using a UV-1601 spectrometer (Shimadzu). X-ray diffraction data were collected using a Rigaku Miniflex instrument

---

(23) (a) Tao, A.; Kim, F.; Hess, C.; Goldberger, J.; He, R.; Sun, Y,; Xia, Y.; Yang, P. *Nano Lett.* **2003**, *3*, 1229. (b) Gunawidjaja, R.; Jiang, C.; Peleshanko, S.; Ornatska, M.; Singamaneni, S.; Tsukruk, V. V. *Adv. Funct. Mater.* **2006**, *16*, 2024.

(24) Gao, Y.; Song, L.; Jiang, P.; Liu, L. F.; Yan, X. Q.; Zhou, Z. P.; Liu, D. F.; Wang, J. X.; Yuan, H. J.; Zhang, Z. X.; Zhao, X. W.; Dou, X. Y.; Zhou, W. Y.; Wang, G.; Xie, S. S.; Chen, H. Y.; Li, J. Q. *J. Cryst. Growth* **2005**, *276*, 606.

(25) Sun, Y.; Xia, Y. *Adv. Mater.* **2002**, *14*, 833.

(26) Gao, Y.; Jiang, P.; Liu, D. F.; Yuan, H. J.; Yan, X. Q.; Zhou, Z. P.; Wang, J. X.; Song, L.; Liu, L. F.; Zhou, W. Y.; Wang, G.; Wang, C. Y.; Xie, S. S.; Zhang, J. M.; Shen, D. Y. *J. Phys. Chem. B* **2004**, *108*, 12877.

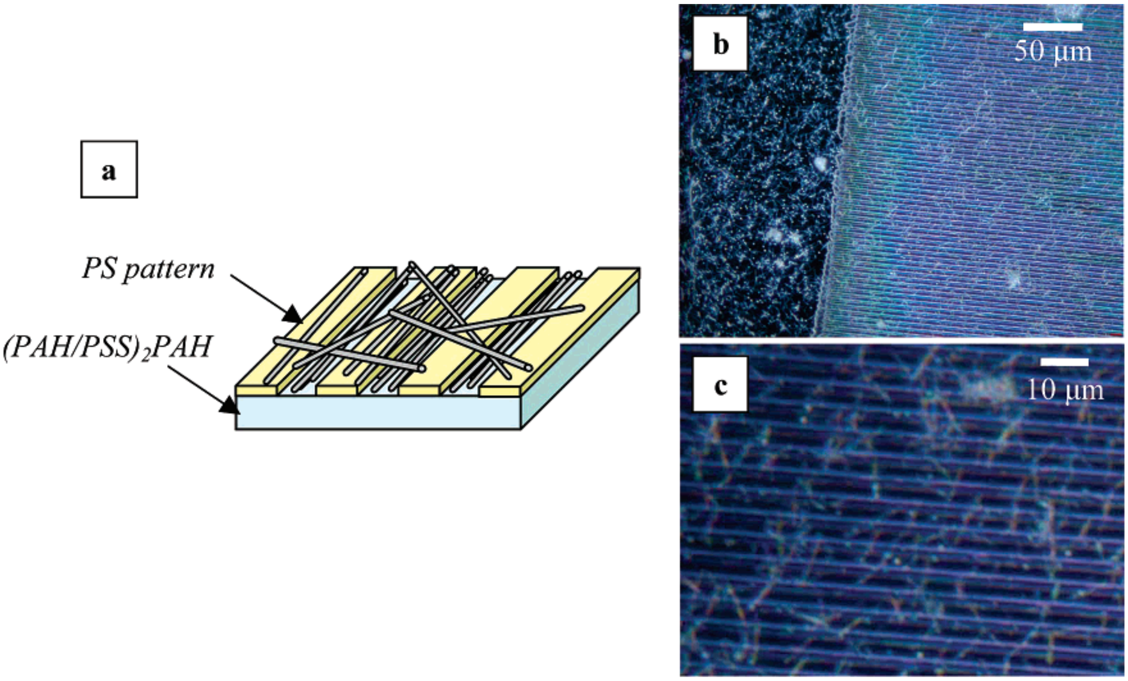

Figure 2. (a) AgNWs cast on the PS micropatterned surface. Optical images were obtained in dark-field mode (b and c).

with Cu Kα radiation ($\lambda = 0.154$ nm) between $2\theta = 10°$ and $2\theta = 90°$. The surface behavior at the air−water interface and LB monolayer deposition onto silicon and glass substrates were conducted at room temperature using a KSV-2000 LB minitrough according to the usual procedure.[27] AgNWs were deposited from the 3 mg/mL chloroform solution (HPLC grade) in 60−100 μL volume uniformly distributed onto the water surface (Nanopure, 18 MΩ cm). It was allowed to evaporate and spread evenly over 30 min. LB depositions onto either of these substrates were performed at a rate of 1 mm/min. Rectangular glass slides (Fisher Scientific) and the [100] silicon wafers with 100−200 nm SiO_2 layers (International Wafers Co.) were chemically treated with "piranha solution" (30:70 hydrogen peroxide/sulfuric acid mixture: *hazardous solution!*) for 1 h to remove contaminations, abundantly rinsed with Nanopure water, and dried with a nitrogen stream. All procedures were conducted in a cleanroom class 100.

Poly(allyamine hydrochloride) (PAH, M_w = 70 000) and poly(styrene sulfonate) (PSS, M_w = 70 000) were purchased from Aldrich and used as received for the spin-assisted assembly of LbL films as described elswhere.[28] Oriented AgNWs were sandwiched between two 10-bilayer PAH/PSS films to give the ultrathin composite film with the effective thickness below 50 nm[23] which can be described as $(PAH/PSS)_{10}$PAH-Ag-$(PAH/PSS)_{10}$PAH, or Ag-LbL for short. This film was fabricated on a thick SiO_2 sacrificial layer to allow for support to be removed and film to be released.

Surface morphology of these films was examined using atomic force microscopy (AFM), scanning electron microscopy (SEM), and optical microscopy (OM). AFM images were collected using a Dimension-3000 microscope in the "light" tapping mode according the usual procedure.[29,30] WSxM software was used for analysis and data representations of AFM images.[31] SEM was conducted in a secondary electron scattering mode at 20 kV (JSM-6060LV). Optical images were captured using a Leica MZ16 microscope in a reflection mode. Angular orientation and the length distribution of 1000 nanowires within three selected surface areas (100 × 100 μm^2) were measured by defining two coordinate points per a single nanowire using a program written in Visual Basic Net. This analysis also yields the number of AgNWs per a given surface area thus allowing the evaluation of their volume fraction.

For the anisotropic buckling test, the Ag-LbL film was transferred on an elastic poly(dimethylsiloxane) (PDMS) substrate (0.6 cm × 0.6 cm × 0.4 cm), and the compressive force was exerted perpendicular and parallel to AgNW orientation at micrometer-size increments. Fourier transformations of these images were done with *ImageJ* to estimate the buckling spacing. Copper pinholes and transmission electron microscopy (TEM) grids (200 meshes) were purchased from Electron Microscopy Sciences.

Results and Discussion

Highly Oriented AgNWs on Micropatterned Silicon. Initially, AgNW orientation was conducted by a tilted drop casting of the AgNW solution (1−3 mg/mL in methanol) onto an array of narrow channels composed of a sacrificial polystyrene (PS) micropattern (ridges with 3 μm periodicity and 1 μm height). This pattern prior to this was covered by $(PAH/PSS)_2$PAH LbL film to ensure proper anchoring properties (Figure 2a). This technique was successfully used for the fabrication of patterned carbon nanotube arrays as discussed elsewhere.[32,33] It is expected that, as methanol evaporates, the stiff AgNWs whose length (~6 μm) is greater than the width of PS ridges are confined and forced to orient in the direction parallel to these ridges.

The initial optical image shows no direct evidence of AgNWs "trapped" in the microchannels with a fraction of

---

(27) Ulman, A. *An Introduction to Ultrathin Organic Films: From Langmuir-Blodgett to Self-Assembly*; Academic Press: Boston, MA, 1991.

(28) Jiang, C.; Markutsya, S.; Tsukruk, V. V. *Adv. Mater* **2004**, *16*, 157.

(29) Tsukruk, V. V. *Rubber Chem. Technol.* **1997**, *70*, 430.

(30) Tsukruk, V. V.; Reneker, D. H. *Polymer* **1995**, *36*, 1791.

(31) Horcas, I.; Fernandez, R.; Gomez-Rodriquez, J. M.; Colchero, J.; Gomez-Herrero, J.; Baro, A. M. *Rev. Sci. Instrum.* **2007**, *78*, 013705.

(32) Ko, H.; Jiang, C. Y.; Shulha, H.; Tsukruk, V. V. *Chem. Mater.* **2005**, *17*, 2490.

(33) (a) Ko, H.; Peleshanko, S.; Tsukruk, V. V. *J. Phys. Chem. B* **2004**, *108*, 4385. (b) Ko, H.; Jiang, C. Y.; Tsukruk, V. V. *Chem. Mater.* **2005**, *17*, 5489.

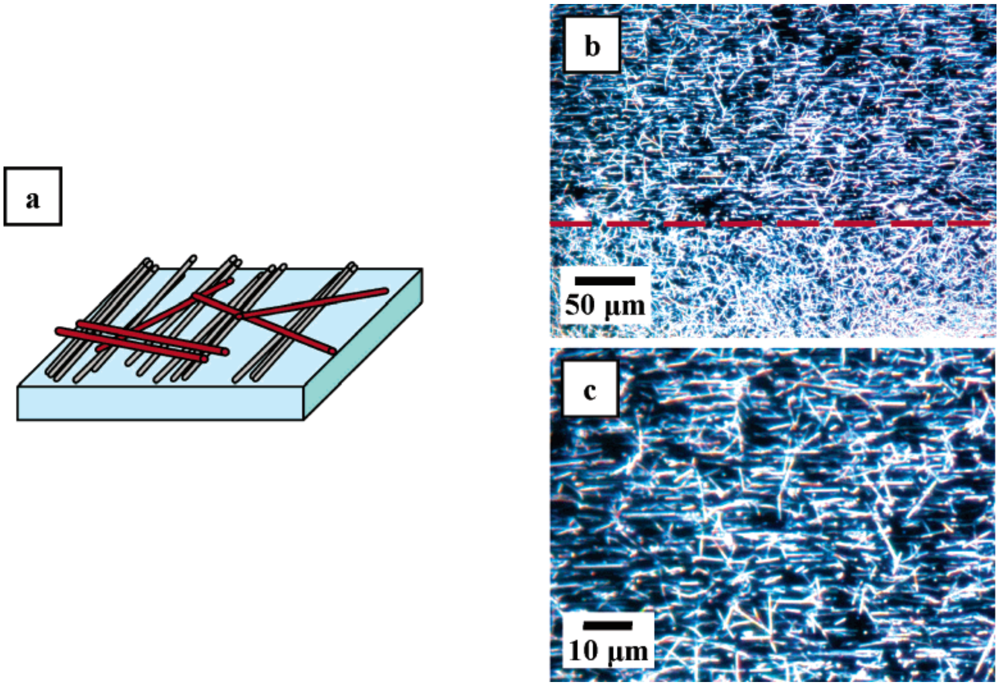

Figure 3. (a) AgNWs cast on PS micropatterned surface after removal of PS pattern. Optical images were obtained in dark-field mode (b and c). Dotted line represents the interface between oriented and random AgNWs on the unpatterned surface.

randomly distributed AgNWs on top of the PS micropattern and outside of the patterned area (Figure 2b,c). However, a consequent removal of the PS ridges by dissolution on toluene shows a large fraction of highly oriented AgNWs (Figure 3). The dotted line in Figure 3b separates the patterned and non-patterned surface areas showing the effectiveness of the microprinting-assisted AgNW orientation with, however, some unoriented fraction still present. The absence of AgNWs prior to PS ridges removal can be related to the fact that the AgNWs were "concealed" along the corners of the microchannels which resulted in a low optical contrast.[34]

Ag-PVP-PEO Nanowires within Langmuir and LB Monolayers. Alternatively, poly(ethylene glycol) methyl ether DL-6,8-thioctate treated AgNWs were placed at the air–water interface and oriented by directional compression. Chemical modification of AgNWs with water soluble PEO chains was critical for inducing the amphiphilic behavior. These modified nanowires display a stable Langmuir isotherms under compression up to about 50 mN/m surface pressure (Figure 4). A reversible behavior was observed within the liquid state at the low surface pressure $P < 5$ mN/m.[35,36] The overall isotherm shape suggests the stable amphiphilic behavior after modification with the PEO chains with an initial gradual increase in the surface pressure to be attributed to the submerging of the PEO chains into the water subphase.[37,38] The steep increase in the surface pressure was detected for the surface areas below 11 μm^2 per nanowire (Figure 4a).

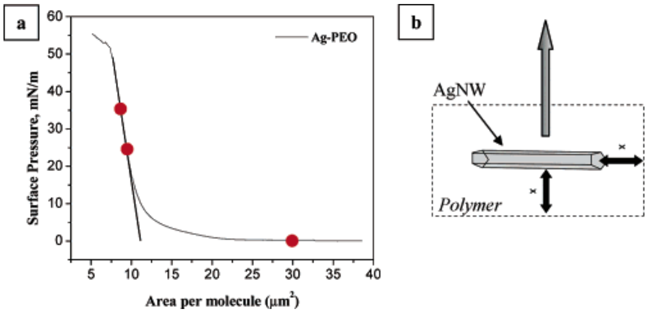

Figure 4. (a) Langmuir isotherm of Ag-PEO nanowires, dots indicate the surface pressures at which depositions were performed. (b) Schematic representation of the surface area occupied by a single nanowire, A_0. Vertical arrow represents the dipping direction.

From Langmuir isotherms, the limiting area, A_0, 11 μm^2, was determined at the steep rise in the surface pressure. On the other hand, at $P = 25$ mN/m, the surface coverage with AgNWs was 3.0 ± 0.6% as determined by counting the number of nanowires in the selected surface areas while using their average length and diameter. The surface area occupied by a single nanowire divided by A_0 yields the surface coverage of 4.0%, which is consistent with the independent image analysis conducted after transfer to the solid support. Some difference is the result of the Ag-PEO monolayer not fully transferred onto the substrate as a result of "cracking" and other defects (see below). Assuming a uniform spacing between AgNWs, the surface area per a single nanowire is estimated to be 1430 nm^2 which is much larger than that estimated for a PEO-modified nanowire using the limiting area of 0.28 nm^2 per a monomeric unit of ethylene oxide (Figure 4b).[39] On the other hand, by taking the limiting area of *N*-vinyl pyrrolidone monomer as 0.1 nm^2, the calculated

---

(34) Messer, B.; Song, J. H.; Yang, P. *J. Am. Chem. Soc.* **2000**, *122*, 10232.

(35) Shan, J.; Nuopponen, M.; Jiang, H.; Viitala, T.; Kauppinen, E.; Kontturi, K.; Tenhu, H. *Macromolecules* **2005**, *38*, 2918.

(36) Fauré, M. C.; Bassereau, P.; Lee, L. T.; Menelle, A.; Lheveder, C. *Macromolecules* **1999**, *32*, 8538.

(37) Peleshanko, S.; Jeong, J.; Gunawidjaja, R.; Tsukruk, V. V. *Macromolecules* **2004**, *37*, 6511.

(38) Gunawidjaja, R.; Peleshanko, S.; Tsukruk, V. V. *Macromolecules* **2005**, *38*, 8765.

(39) Peleshanko, S.; Gunawidjaja, R.; Petrash, S.; Tsukruk, V. V. *Macromolecules* **2006**, *39*, 4756.

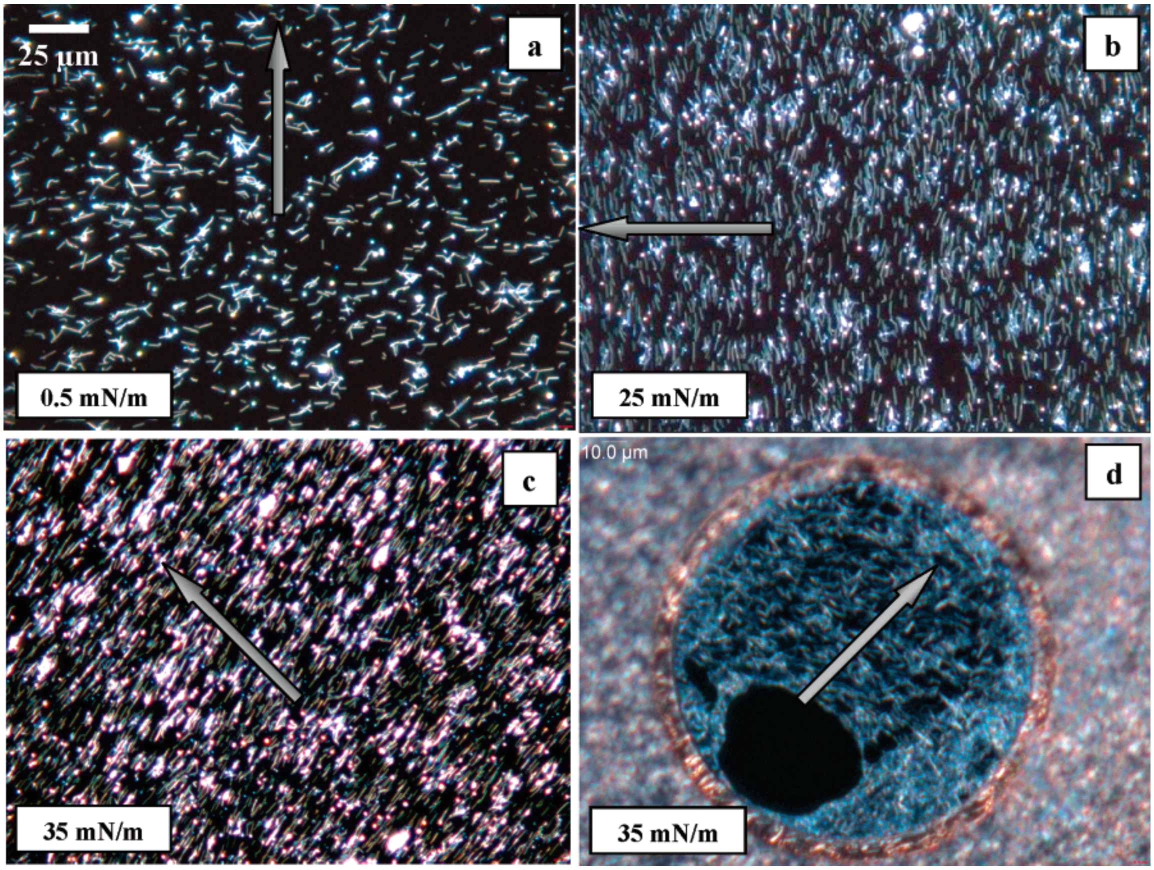

Figure 5. (a) Randomly oriented Ag-PEO nanowires deposited at low surface pressure. (b and c) Unidirectional orientation of Ag-PEO nanowires deposited at different surface pressures. (d) Unidirectional orientation Ag-PEO nanowires deposited over a 150 μm hole. Arrows represent the dipping direction. Scale bar is identical for all images.

surface area occupied by PVP, 1170 nm^2, is estimated to be close to the experimental value indicating that PVP chains control the monolayer compression in the solid-state even after modification with PEO chains.[26,40]

The Langmuir monolayer with AgNWs was deposited on the silicon wafers at three different surface pressures, $P =$ 0.5, 25, and 35 mN/m (Figures 4 and 5). As we observed, the nanowires were randomly distributed at very low pressure, $P = 0.5$ mN/m, but at $P = 25$ and 35 mN/m they become orientated parallel to LB barriers or perpendicular to the dipping direction (represented by arrows in Figure 5). This type of orientation is the well-known phenomenon for rod-like structures often compared to the behavior of rafted logs on a river.[1,11,12] Highly packed AgNWs showing excellent orientation are usually seen at the top of the silicon wafer, but uniformity gradually decreases toward the bottom of the wafer due to the meniscus formed along wafer/water during dipping, a common behavior for the PEO-containing material (Figure 6a).[36,37] Closer examination of LB monolayers reveals occasional anisotropic voids with AgNWs oriented along their boundaries (Figure 6b,c). AFM cross-sectional analysis yields the monolayer thickness of 3.5 ± 1 nm in the regions free of nanowires (Figure 6d). Despite these occasional defects, the Ag-PEO monolayer at the highest surface pressure can be picked up on a copper plate with a pinhole with a 150 μm diameter (Figure 5d). The successful transfer of these monolayers indicates a fairly stable structure (although with some defects, such as big holes) with the overall strength sufficient to be freely suspended over the hole over extended periods of time.

Angular orientation of the individual AgNWs on the surface was compared for two different fabrication procedures by tabulating the angular distribution of nanowires from optical images (Figure 7). From this data, we conclude that the LB-assisted orientation of AgNWs results in much higher level of unidirectionality. The estimated angular disorientation reaches 24° for pattern-assisted cast orientation with significant (about 1/3) fraction of randomly oriented nanowires. The angular disorientation drops to 17° for the LB-assisted routine with no nanowires deviating more than 30° from the orientation direction (Figure 7). Therefore, LB deposition was far more efficient in achieving the highly oriented nanowire array, and this routine was selected as a central step in further fabrication of ultrathin polymer films with encapsulated nanowire arrays.

Freely Suspended Polymer Films with Encapsulated AgNWs. An array of uniaxially oriented AgNWs was deposited at $P = 25$ mN/m in between two (PAH/PSS)$_{10}$ LbL films assembled on a 200 nm thick SiO$_2$ layer, to form the supported Ag-LbL film (Figure 8a). The films were released by dissolving the SiO$_2$ layer in 5% hydrofluoric acid solution (*hazardous solution!*).[41] The released films were transferred into another Petri dish containing acetone via

---

[40] Smith, J. N.; Meadows, J.; Williams, P. A. *Langmuir* **1996**, *12*, 3773.

[41] Olek, M.; Ostrander, J.; Jurga, S.; Moehwald, H.; Kotov, N.; Kempa, K.; Giersig, M. *Nano Lett.* **2004**, *4*, 1889.

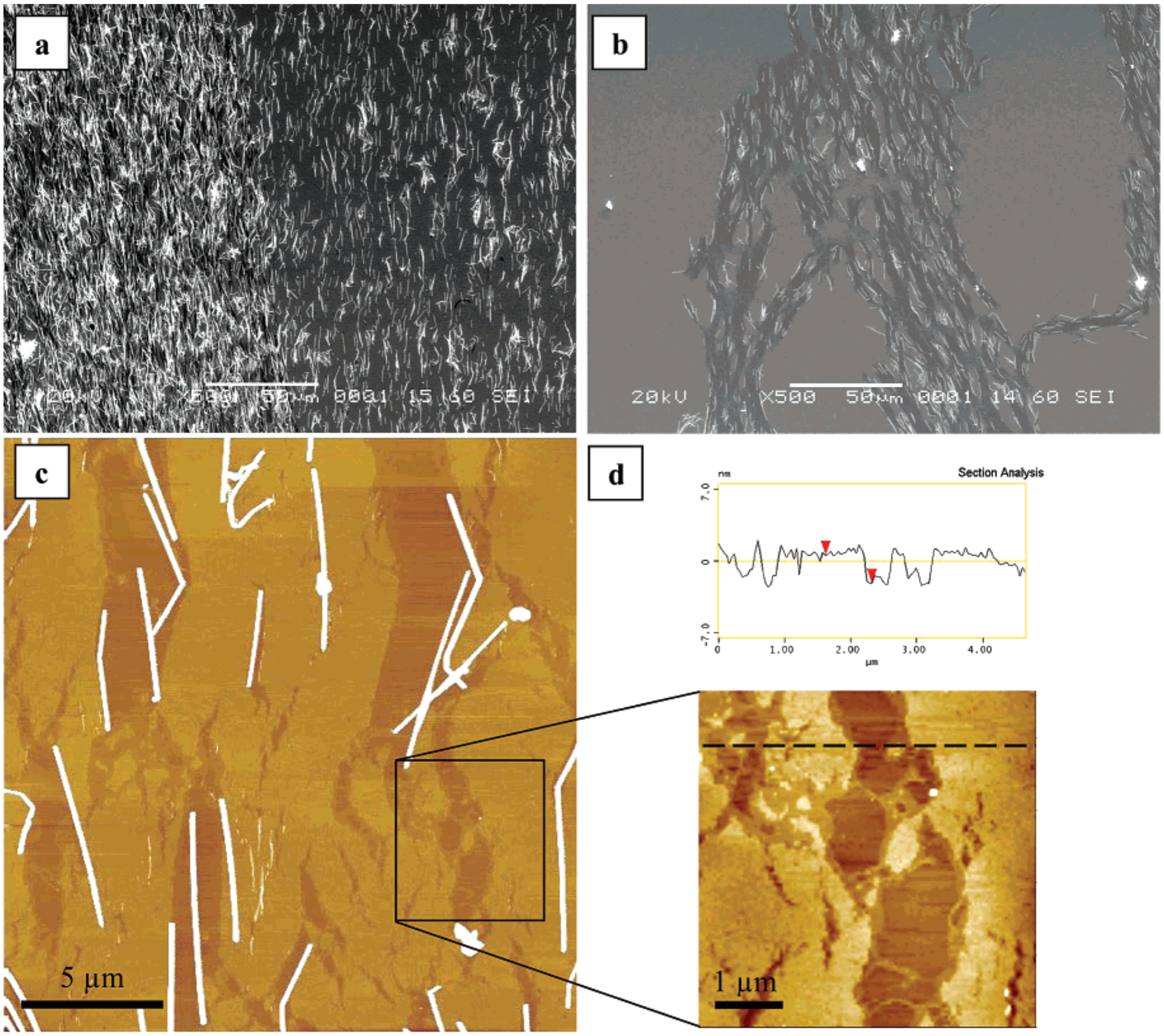

Figure 6. Ag-PEO nanowire monolayers deposited on a silicon wafer. SEM images for monolayer deposited at $P = 25$ mN/m at the (a) top and (b) bottom of the wafer ($P = 35$ mN/m). (c and d) AFM images of monolayer deposited at $P = 35$ mN/m with its corresponding cross-sectional analysis.

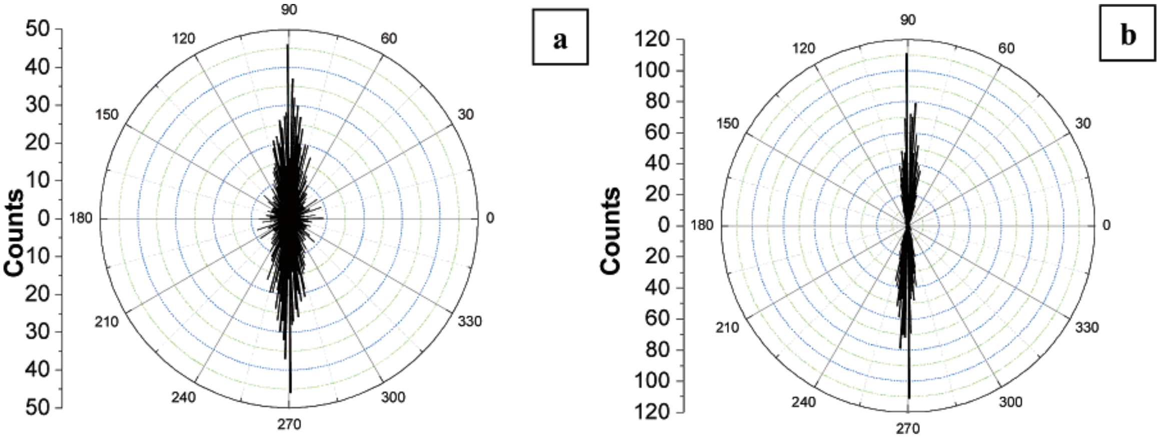

Figure 7. Angular distribution of nanowire orientations (deg), *Y* axis is count for micropattern-assisted (a) and LB-assisted ($P = 25$ mN/m) (b) orientations.

pipet and back into a fresh pool of nanopure water. Upon release from the SiO_2 sacrificial layer, LbL films were strong enough to survive the release and transfer procedures and, moreover, can be freely suspended for a long time preserving nanowire orientation, as demonstrated with a TEM copper grid (Figure 8b). Ag-LbL film deposited on a quartz substrate was used for UV−vis measurement in comparison with the solution state (Figure 9). AgNW solution has an absorption peak at 350 nm (with a shoulder around 380 nm), where the former resembles the bulk silver and the latter corresponds to the transversal plasmon mode.[23] For LbL films, a very similar shape is observed with the main peak around 359 nm with a minor blue shift indicating changing environment.

Anisotropic Mechanical Behavior of LbL Film with Encapsulated Oriented Nanowires. To test the mechanical properties of ultrathin LbL films, they were deposited on the PDMS substrate and the compressive stress was applied both parallel and perpendicular to the orientation of AgNWs

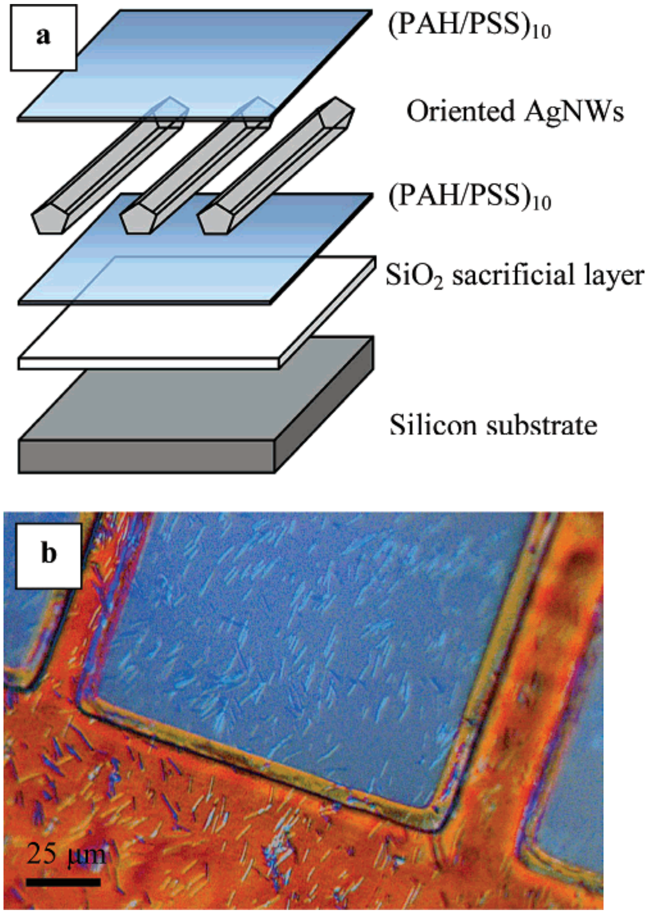

Figure 8. (a) Fabrication of oriented AgNWs sandwiched between two $(PAH/PSS)_{10}$ LbL films on a SiO_2 sacrificial layer. (b) Ag-LbL film suspended over the TEM grid.

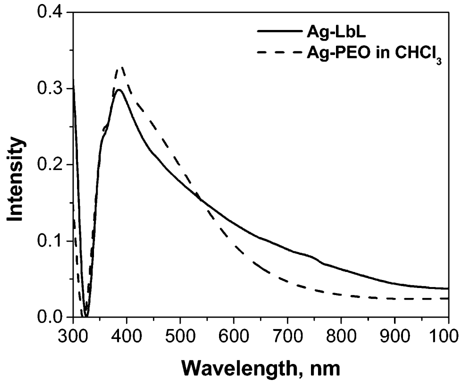

Figure 9. UV−vis spectra of Ag-PEO nanowires in solution and encapsulated within LbL film.

(Figure 10a). For both experiments, we observed long-range buckling instability patterns which differ by spacing and distribution of wrinkles (Figure 10b,c). For the perpendicular compression, the buckling spacing, λ, was 2.6 ± 0.24 μm, while for the parallel compression, the average buckling spacing decreased to 1.5 ± 0.15 μm. It is worth noting that while for parallel compression the buckling spacing is more or less uniform, for perpendicular compression buckling spacings are sporadic and localized in the regions where AgNWs directly oppose the compressive stress. This agrees with the observation of the two-stage buckling phenomenon for the micropatterned encapsulated gold nanoparticle array composite films composed of regions with different stiffness.[42] This observation justified the application of the buckling theory to the composite films for the evaluation of the local mechanical properties because of the highly superpositional nature of buckling instabilities occurring independently in regions with different local properties.

The application of the buckling instability theory yields the Young's modulus of 0.73 ± 0.5 GPa for the direction perpendicular to the nanowire orientation with much higher value of 3.82 ± 0.5 GPa obtained for the direction along the nanowire orientation. Using the Young's modulus for bulk silver, 88 GPa,[43] and the Young's modulus of unfilled PAH/PSS polyelectrolyte film, 1.0 GPa,[15] the theoretical Young's modulus of the composite film can be calculated both in the longitudinal and transverse directions using the Halpin−Tsai equation for anisotropic fiber reinforced composites.[44] These calculations yield $E_T = 1.10$ GPa and $E_L = 2.95$ GPa for transversal and longitudinal directions, respectively, in close agreement with the experimental data.

Buckling of AgNWs. It is logical to expect that upon buckling in the longitudinal direction AgNWs with the elastic modulus 2 orders of magnitude higher than that the polymeric matrix will keep their shape intact. However, optical images showed that the wrinkles were concentrated along the nanowires, an intriguing distribution (Figure 10). Thus, to understand what takes place during buckling in longitudinal directions, LbL films were imaged with AFM while being subjected to the compressive force. For longitudinal buckling, AFM imaging reveals that the AgNWs closely follow the undulated shape of the wrinkle pattern (Figure 11a,c). The AgNWs are indeed buckled with amplitude exceeding 100 nm (Figure 11b). This is the well-known phenomenon which is observed in bulk unidirectional, fiber-reinforced composites when subjected to significant compression loading. Fiber buckling in the bulk can in fact occur when the matrix stresses are in the elastic range for sufficiently low fiber volume fraction (<40%).[44] As a result of AgNW confinement to the interior of the planar LbL film, even minor compressive strain below 0.2% initiates the nanowire buckling with two to three smooth modulated segments per nanowire (Figure 11).

To elucidate if the compressive stress transferred by the polymer matrix is sufficient to deform AgNWs, we estimated the stress developed by the compressed PDMS substrate and compared this value with that needed to initiate the buckling instability of a column derived from Euler's equation:[45,46]

$$\sigma_{\text{critical}} = F/A = \left[\frac{(K\pi^2 E_{\text{AgNW}} I)}{l^2}\right]/(\pi r^2) \qquad (1)$$

with $K = 4$ (for a column fixed ends), I is the moment of inertia, l is the average nanowire length, and r is its average

---

(42) Jiang, C.; Singamaneni, S.; Merrick, E.; Tsukruk, V. V. *Nano Lett.* **2006**, *6*, 2254.

(43) Li, X.; Gao, H.; Murphy, C. J.; Caswell, K. K. *Nano Lett.* **2003**, *3*, 1495.

(44) Agarwal, B. D.; Broutman, L. J. *Analysis and Performance of Fiber Composites*, 2nd ed.; Wiley: New York, 1990; p 92.

(45) Volynskii, A. L.; Bazhenov, S.; Lebedeva, O. V.; Bakeev, N. F. *J. Mater. Sci.* **2000**, *35*, 547.

(46) Hibbeler, R. C. *Mechanics of Materials*, 4th ed.; Prentice Hall: New York, 2000; p 652.

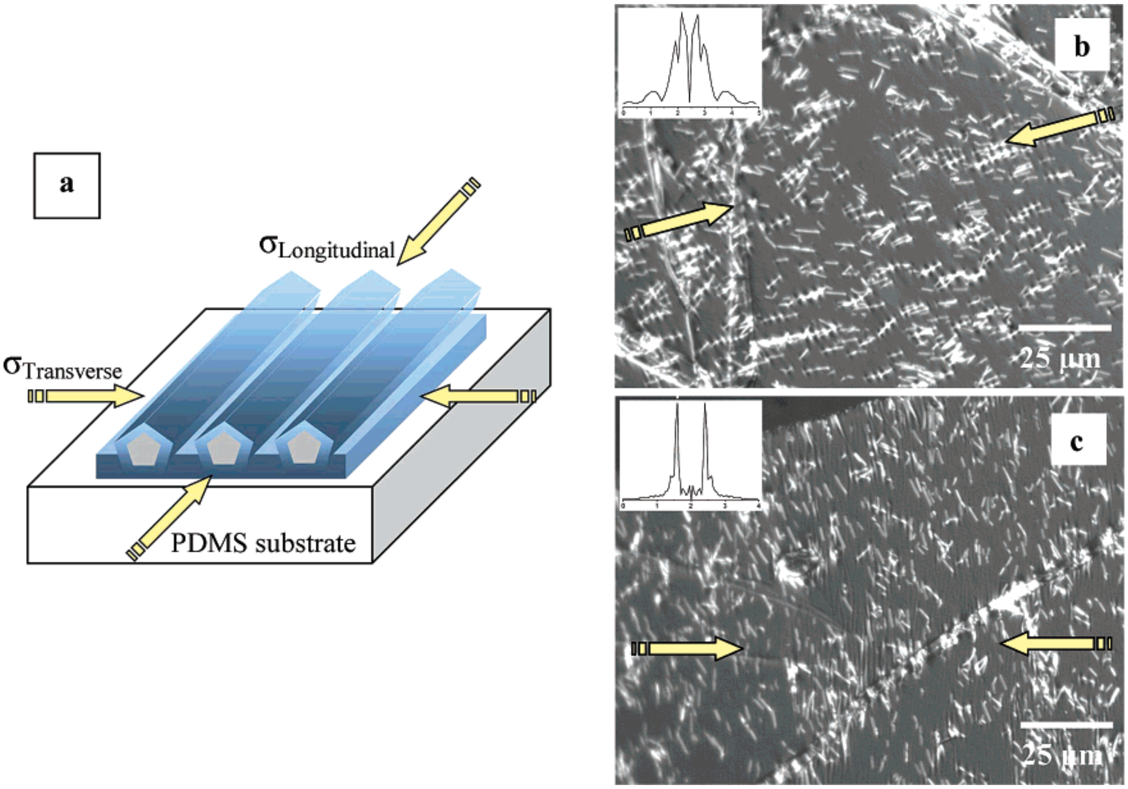

Figure 10. LbL film deposited on PDMS substrate and buckled in the longitudinal and transversal directions (a) and corresponding optical images (b, c). Insets are a representative 1D fast Fourier transforms for selected cross sections of buckled nanowires. X axis is $1/\lambda$ ($1/\mu$m).

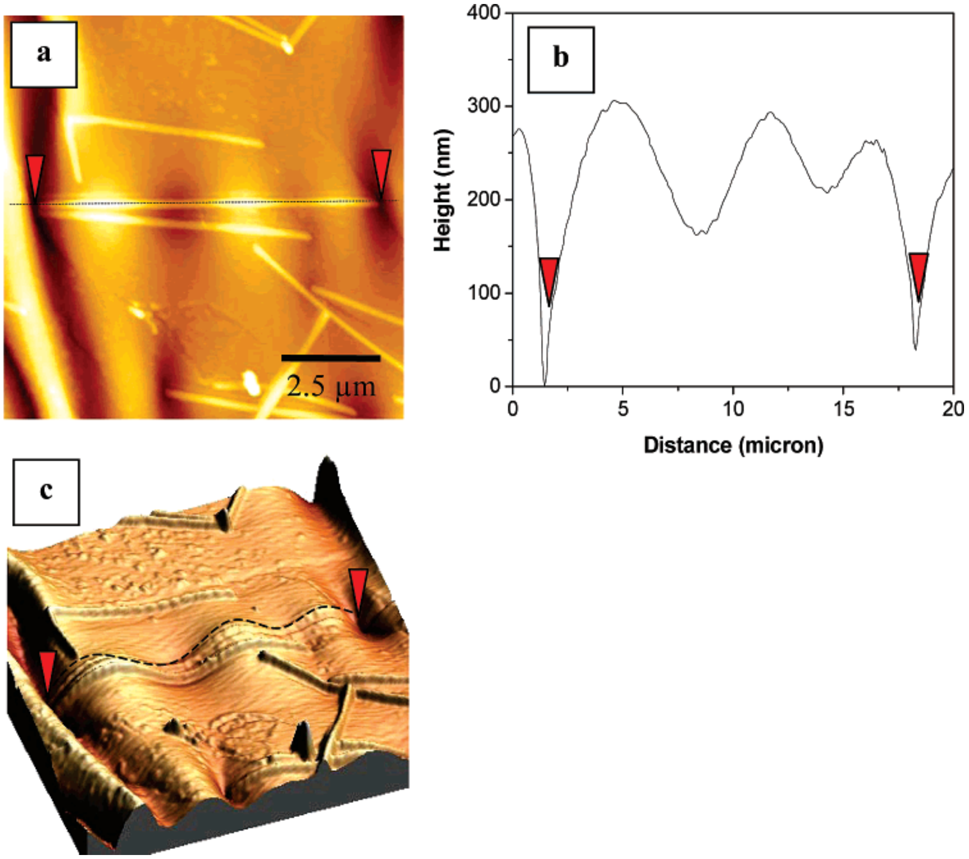

Figure 11. AFM images of Ag-LbL film buckled in the longitudinal direction, height is 500 nm, (a, c) and corresponding cross-section profile along a single buckled nanowire (along dotted line) (b). Red arrows mark the two ends of the undulated nanowire.

radius. This analysis confirmed that the compression stress developed by the polymer matrix can cause the nanowire buckling.

Moreover, from this analysis we directly evaluated the elastic modulus of the AgNW in the longitudinal direction $E_{\mathrm{AgNW}} = 118 \pm 14$ GPa. This value is close to the 124 GPa determined for the (100) direction of silver single crystal[47] and within the range of elastic moduli determined by direct buckling of an individual nanowire from corresponding force-displacement measurements, 100−120 GPa.[48] However, this number is higher than that usually measured for the bulk silver as well as one measured for AgNWs by nanoindentation (83−88 GPa).[42] The higher Young's modulus of AgNW having penta-twinned cross section compared to bulk silver can be related to the grain boundary hardening effect imposed by the nanowire lateral facets as suggested earlier.[47] Some differences could also be ascribed to the role of surface stiffness and different directions of mechanical deformations.[49] The phenomenon of the buckling of the AgNWs encapsulated into ultrathin polymer film by the application of the compressive stress along their long axis represents the straightforward and fast way for the evaluation of the elastic properties of the metal nanowires by measuring their buckling periodicity.

Acknowledgment. This work is supported by AFOSR FA9550-05-1-0209 and NSF-NIRT-0506832 grants. The authors thank Dr. Sergiy Peleshanko for meaningful discussions and technical support.

CM063022E

---

(47) Cao, Y.; Allameh, S.; Nankivil, D.; Sethiaraj, S.; Otiti, T.; Soboyejo, W. *Mater. Sci. Eng. A* **2006**, *427*, 232.

(48) Wu, B.; Heidelberg, A.; Boland, J. J.; Sader, J. E.; Sun, X.; Li, Y. *Nano Lett.* **2006**, *6*, 468.

(49) Cuenot, S.; Frétigny, C.; Demoustier-Champagne, S.; Nysten, B. *Phys. Rev. B* **2004**, *69*, 165410.